

Conductivity Studies in Europium Oxide[†]

M. R. Oliver, *[‡] J. O. Dimmock, A. L. McWhorter, * and T. B. Reed
Lincoln Laboratory, Massachusetts Institute of Technology, Lexington, Massachusetts 02173
 (Received 3 March 1971)

The electrical and optical properties of EuO are studied in order to help determine conduction mechanisms. A strong relationship between growth parameters and electrical behavior is noted. Free-carrier absorption below the band edge in energy is observed in moderately conducting crystals. By comparing optical and electrical results, an experimental determination is made of carrier-density and scattering-time contributions to resistivity behavior. The carrier-density variations are explained in terms of an earlier proposed model which is developed here. The model consists of a donor-trap level, believed to be caused by an oxygen vacancy, which is above the conduction-band edge at low temperature, but crosses below it (near 50 °K) with increasing temperature. Magnetoresistance and pressure results are presented which strongly support the model.

I. INTRODUCTION

EuO is one of the most extensively investigated of those compounds that are both ferromagnetic and semiconducting.¹ Until recently, however, these investigations have not encompassed studies of electrical behavior in EuO. Most of the electrical-behavior investigations in ferromagnetic semiconductors have been carried out on the Eu chalcogenides EuS and EuSe, and on the chalcogenide spinels CdCr₂S₄ and CdCr₂Se₄.

Suits² first discovered anomalous resistivity effects in ferromagnetic semiconductors when he observed a resistivity peak near the Curie temperature in doped EuS. Heikes and Chen³ published the first resistivity as a function of temperature curves. These studies indicated an unusual dependence of the resistivity on doping. Considerable amounts (1–10%) of doping with other rare earths (e.g., La or Gd) appeared to be necessary for substantial conductivity. Later, von Molnar and Methfessel⁴ observed a giant magnetoresistance associated with the resistivity peak in EuSe. Lehmann⁵ has investigated similar effects in the chalcogenide spinels. In all the ferromagnetic semiconductors, the mobility, when measurable, is quite low. The observation of many unusual effects has led to further investigation concerning the nature of electrical conductivity in these compounds.

Several mechanisms have been proposed for the conduction processes in ferromagnetic semiconductors. Critical scattering theories for band electrons have been proposed and discussed by several authors.^{6–8} Kasuya and Yanase⁹ have proposed a magnetically limited hopping mechanism, and for sufficient impurity densities, conduction in an impurity band. In earlier work on these materials, it appeared that large amounts of dopants had to be added to the compound to get significant conductivity. The observation was consistent with conduc-

tion in a partially compensated impurity band.

As a material for conductivity investigations, EuO would appear to have an advantage over the other europium chalcogenides. Its high Curie point (69.5 °K for EuO versus 16.9 °K for EuS and 4.6 °K for EuSe)¹⁰ should allow more effective separation of phenomena associated with temperature regions below, near, and above the Curie point. These potential advantages were outweighed until recently by the difficulties involved in growing suitable single crystals of EuO.

Because of the problems associated with single-crystal growth in the Eu chalcogenides, many of the first experiments were done on powders and polycrystalline material. Guerci and Shafer¹¹ found, however, that single-crystal EuO could be grown by sealing Eu metal and Eu₂O₃ in a tungsten crucible and heating to temperatures above the melting point and then cooling the crucible slowly. The melting point, as recently determined by Reed and Fahey,¹² is (2270 ± 20) °K. The method of Guerci and Shafer is essentially that used for growing crystals which have been used for this investigation. Another growth method, that of Kaldis,¹³ employs vapor transport and also produces crystals of high quality. The details and problems of the crystal growth process are reported elsewhere.¹² Except for the lowest-resistivity samples ($\rho_{\text{room temp.}} < 10^{-2} \Omega \text{ cm}$), the material used in our investigation was not intentionally doped.

II. EXPERIMENTAL RESULTS

This project was initiated in order to investigate the conduction processes in EuO. To that end, a major portion of the experimental studies were devoted to measurement of the resistivity as a function of several parameters: temperature, magnetic field, and pressure. These measurements were made on samples of varying resistivity level. Optical-absorption measurements were also

carried out. Measurements of the absolute transmission as a function of wavelength were made below the band edge in energy.

The resistivity was measured using the van der Pauw¹⁴ technique. Sample thicknesses ranged from 50 to 800 μ , and the other dimensions from 1 to 4 mm. The ρ vs T measurements were made in an exchange gas Dewar using a platinum resistor as a thermometer above 20°K and a germanium resistor below 20°K. The magnetoresistance measurements were made with a superconducting magnet, capable of achieving fields up to 50 kG. The pressure apparatus was described in an earlier report.¹⁵

The optical-absorption experiments were carried out using a dual-beam two-channel system. The transmission of the material was measured by comparing the light transmitted through a path that includes the sample with the light transmitted through a reference channel. By using chopping techniques only one detector was used, and narrow-band lock-in voltmeters were employed to detect the transmitted signals. The outputs of the lock-in voltmeters were fed to a ratiometer whose output was recorded.

Electrical contacts were made using an alloy suggested by von Molnar based on the La-rich La-

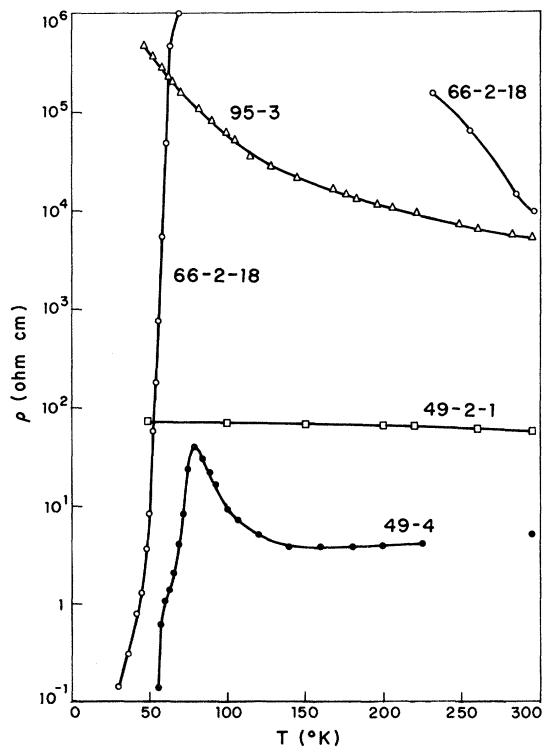


FIG. 1. Four resistivity-vs-temperature curves for EuO. Curves for samples 66-2-18 and 49-4 represent type-A behavior; those of 95-3 and 49-2-1, type-B behavior (see text).

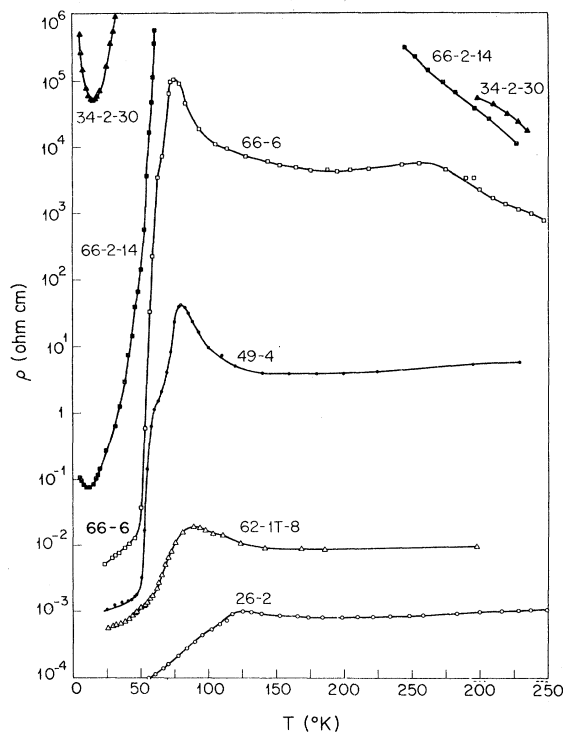


FIG. 2. Resistivity vs temperature for representative type-A EuO samples showing change of behavior with increasing conductivity level.

Ag eutectic. The alloys were applied by heating in an atmosphere of Ar or He.

A. Temperature Dependence of Resistivity

In examining the temperature dependence of the resistivity, we found that two distinctly different types of resistivity behavior occur in EuO. Two examples of each type are shown in Fig. 1. Two of the curves, 49-4 and 66-2-18, exhibit a large resistivity peak in the vicinity of the Curie point. This resistivity type, which we will call type A, has been observed in EuO previously by von Molnar and Shafer,¹⁶ and also in the other europium chalcogenides. A second type of behavior, which we will call type B, is exhibited in curves 49-2-1 and 95-3. These resistivity curves show no anomaly associated with the magnetic phase transition. Instead, the resistivity increases slowly and monotonically with decreasing temperature. The higher-resistivity type-B curves show a larger temperature variation. This type of resistivity behavior has apparently been observed by Samokhvalov *et al.*¹⁷

The curves of Fig. 1 are all for undoped crystals and are representative of behavior observed in many samples. The resistivity type has been correlated with growth procedures. Type-A behavior occurs in crystals grown from a starting mixture containing an excess of Eu above stoichiometry. Type-B

behavior occurs in material grown from stoichiometric amounts of starting materials. Another difference between the two types is that type-*A* material gives an *n*-type thermoelectric power while type *B* gives no measurable reading. Most of the work reported here is on type-*A* material, and unless otherwise specified, all subsequent data will refer to type-*A* material.

Depending upon the amount of doping, intentional or otherwise, and upon deviations from stoichiometry, EuO can exhibit a very wide range of resistivity behavior. Six representative curves that span most of our experimentally accessible range are shown in Fig. 2. It can be seen that the structure of these curves changes considerably in going from the highest-resistivity curve 34-2-30 to the lowest one 26-2. Curves similar to the highest-resistivity curve 34-2-30 and the lowest-resistivity curve 26-2 have been published by von Molnar.^{16,18} Some intermediate curves from the present work have also been previously reported.^{15,19} These curves are typical of the behavior observed in EuO, and exhibit the structure representative of their respective resistivity levels.

The highest-resistivity curve 34-2-30 shows a minimum in resistivity at $\sim 15^\circ\text{K}$. Below the minimum the resistivity increases by over a factor of 10 down to 4.5°K . Above this minimum the resistivity rises very quickly and becomes unmeasurable well below the Curie point. When it becomes measurable again (around 280°K), it exhibits an activation-energy behavior. The activation energy for this curve is $\sim 0.3\text{ eV}$; the values observed in other high-resistivity samples deviate little from this. This type of behavior was first reported by von Molnar.¹⁸ The next highest curve, 66-2-14, shows a much smaller minimum at low temperatures. The resistivity starts at a lower level than 34-2-30, and above the minimum rises more slowly with increasing temperature. At 50°K it exhibits an increase in $d\rho/dT$. At higher temperatures, it also exhibits an activation energy of $\sim 0.3\text{ eV}$. Though the resistivity has decreased relative to that of 34-2-30, the activation energy remains roughly the same.

The next lower curve, 66-6, has several features that sharply contrast with higher-resistivity material. The resistivity increases very slowly with increasing temperature up to 50°K . In sample 66-2-14, $d\rho/dT$ increased, but at 50°K it was already fairly large. In 66-6, the change at 50°K is more dramatic. The resistivity changes by about six orders of magnitude up to 65°K , and appears to round off a little. A peak is observed between 75 and 80°K , well above the Curie point of 69°K . Above the peak the resistivity drops between one and two orders of magnitude to a broad minimum around 160°K . On the scale of Fig. 2, the resistivity remains relatively constant out to about 250

$^\circ\text{K}$, though it is actually rising slowly above 160°K . Near 250°K it changes character, and above 270°K it exhibits an activation-energy behavior with an activation energy of $\sim 0.22\text{ eV}$. This value is somewhat less than that of the two higher-resistivity samples.

Sample 49-4 is the next-lowest-resistivity curve. Its low-temperature behavior is quite similar to that of 66-6. The resistivity is almost flat until 50°K where the elbow in the resistivity is observed. Above this elbow the resistivity increases by about a factor of 500 in a 10°K range. There is further structure in the curve between 60 and 100°K . The curve has a shoulder between 60 and 70°K . The resistivity increases about a factor of 20 from this shoulder to a rounded peak between 75 and 80°K . Above this peak the resistivity decreases about one order of magnitude and reaches a broad minimum between 100 and 200°K . Beyond this minimum it increases very slowly with increasing temperature. This behavior is very similar to that of 66-6, except that there is no observable activation-energy behavior out to 350°K . There is about a one order of magnitude difference in the resistivity between the two curves (49-4 and 66-6) below 50°K , while the difference at 150°K is about three orders of magnitude. Similar behavior occurs throughout the moderate-conductivity range. Small changes in low-temperature resistivity are accompanied by much larger changes in higher-temperature resistivity.

The next-lower-resistivity sample is 62-1T-8. In order to lower the resistivity to the level of this sample and below, it was necessary to intentionally dope the crystals.

For sample 62-1T-8, the dopant was Gd; Gd and La were the typical dopants used in this investigation. To the starting materials 100-ppm (0.01 at.%) Gd was added. Several significant changes occurred as the resistivity level dropped from that of 49-4 to 62-1T-8. First, the sharp elbow at 50°K disappeared and there is a more gradual less-structured rise to the resistivity peak. Second, the peak is shifted upward in temperature to about 90°K . Above the peak the resistivity decrease to the broad trough between 100 and 200°K is less than a factor of 3, while sample 49-4 has a drop of about a factor of 20. Magnetometer measurements by Menyuk on a piece of material taken from the same part of the crystal as 62-1T-8 showed that the Curie point had increased, but from the complex magnetic behavior it was not possible to determine the precise shift. The shift in the resistivity peak appears to follow that of the Curie point, however.

The lowest-resistivity sample in Fig. 2 is sample 26-2. An amount of 2 at.% Gd was added to the starting materials that yielded this sample. The changes that occurred in the transition from the

behavior of sample 49-4 to that of 62-1T-8 occur in more marked degree in sample 26-2. The increase in resistivity at low temperature is much more gradual than in 62-1T-8. The peak in the resistivity is at about 125 °K and is much smaller than in higher-resistivity samples. There is only about a 20% drop above the peak to the minimum, which occurs around 200 °K. Magnetometer studies on material from the same crystal showed a more well-defined Curie point than in 62-1T-8. The Curie point was at about 122 °K. This is quite close to the maximum Curie point reported for material doped with other rare earths.

Summarizing the results shown in Fig. 2, the curves exhibit structure of several kinds. This structure is associated with the resistivity level, high-resistivity material exhibiting different structure from low-resistivity material. Again, all of these curves exhibit type-A resistivity. At high-resistivity levels, there is a low-temperature minimum in the ρ - T curve and an activation energy at higher temperatures. Intermediate resistivity curves have a sharp elbow near 50 °K, with the resistivity at low temperatures (< 150 °K) being much lower than that well above the Curie point. A resistivity peak occurs slightly above the Curie

point and is well rounded. At lower-resistivity levels, as the total change in resistivity from low to high temperatures becomes smaller the Curie point is shifted upward in temperature and the resistivity peak near the Curie point decreases in size.

B. Optical Results and Interpretation in Terms of Free-Carrier Absorption

In Sec. I, mention was made of the low mobilities observed in the Eu chalcogenides, and in magnetic semiconductors in general. Several Hall-effect measurements on highly doped Eu chalcogenides have been reported, and the room-temperature mobilities are on the order of 10 cm²/V sec.²⁰ These materials are ferromagnets and the additional problem of demagnetization is present near and below the Curie point. A further obstacle to making Hall measurements is the difficulty of separating the normal and anomalous Hall coefficients. These and other difficulties combine to make the determination of the mobility throughout the temperature range studied quite difficult. In order to aid in determining the relative contributions to the conductivity of carrier density and mobility, other measurements were considered. One such experiment was

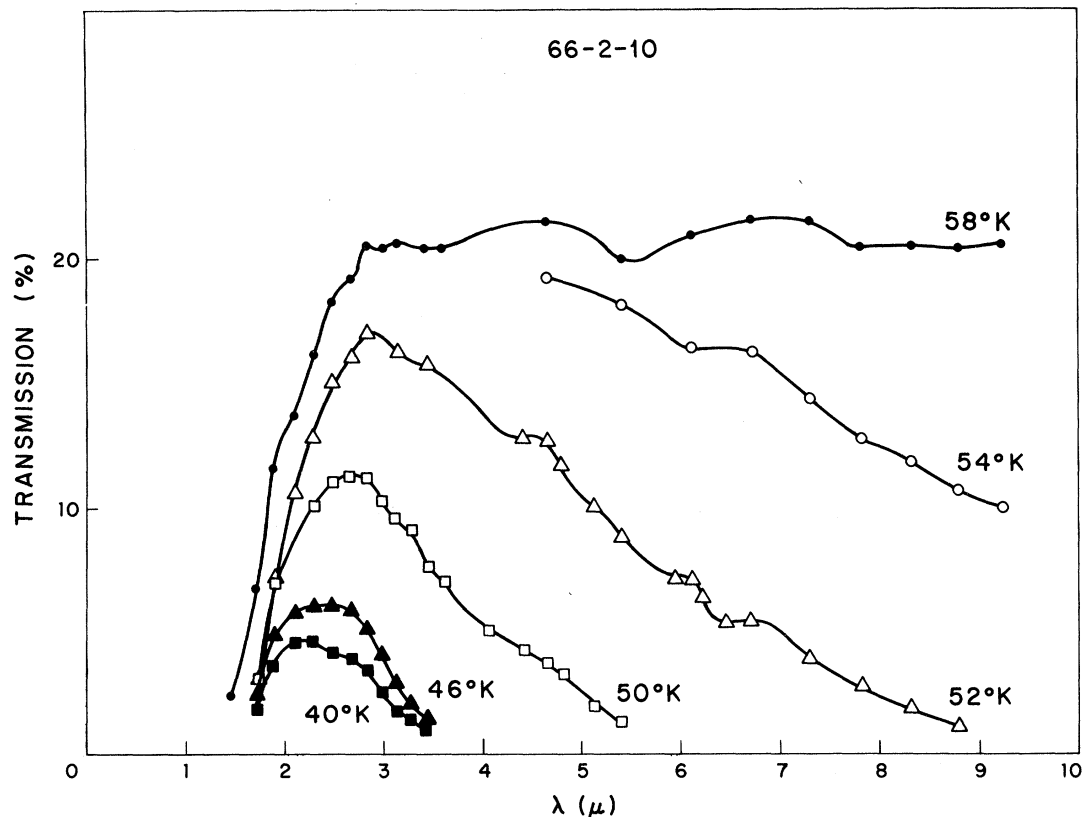


FIG. 3. Transmission vs wavelength for EuO sample 66-2-10. The measurements show the transition in behavior which occurs near 50 °K.

optical absorption below the band-edge energy. Measurements made on conducting samples showed an absorption coefficient that increased with increasing wavelength. The absorption was strongest in the most highly conducting samples and the characteristics suggested the possibility of free-carrier absorption.

A typical set of optical-transmission curves for a moderately conducting sample 66-2-10 is shown in Fig. 3; the resistivity as a function of temperature for the same sample is shown in Fig. 4. For temperatures near and above the Curie point, the optical transmission rises below the band gap and exhibits some structure as a function of wavelength, but does not decrease with increasing wavelength. Free-carrier absorption would only be expected to be observable when it is comparable to absorption from other mechanisms. For this sample, this condition appears to be fulfilled for temperatures around 54°K and below, while above that temperature the transmission is limited by reflection losses and absorption from other mechanisms. The wavelength-dependent absorption sets in around 54°K and increases strongly with decreasing temperature until $T \approx 45^\circ\text{K}$. Below this temperature the absorption levels off and there is no further increase in absorption with decreasing temperature.

In the Drude model the expression for free-carrier absorption is

$$\alpha = \frac{\sigma}{nc\epsilon_0} \frac{1}{1 + \omega^2\tau^2}, \quad (1)$$

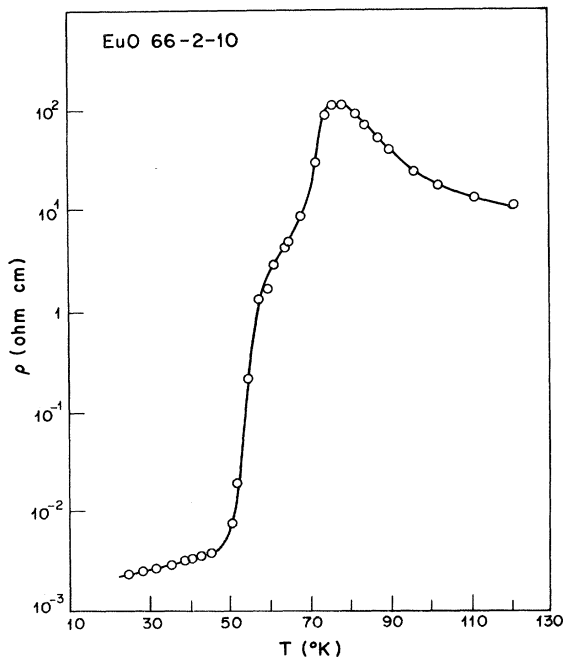


FIG. 4. Resistivity as a function of temperature for sample 66-2-10.

where α is the absorption coefficient, σ the conductivity, n the refractive index, c the velocity of light, and ϵ_0 the permittivity of free space. The angular frequency is given by ω , and τ is the mobility scattering time. In the approximation of $\omega\tau \gg 1$,

$$\alpha = \left(\frac{e^2}{4\pi^2 c^3 n \epsilon_0 m^*} \right) \left(\frac{n_c}{\tau} \right) \lambda^2. \quad (2)$$

Here m^* is the effective mass of the electrons, n_c the conduction-electron density, and λ is the wavelength of the radiation. This expression assumes that τ is energy independent. If, however, $\tau = \tau(E)$, then the λ^2 law is somewhat modified.

By knowing the refractive index n , and assuming a temperature-independent value of m^* , it is possible to evaluate n_c/τ if the absorption coefficient α varies as λ^2 . For sample 66-2-10, α is plotted versus λ^2 for various temperatures in Fig. 5. The variation of α goes slightly more strongly than λ^2 ; it varies roughly as $\lambda^{2.5}$. This is typical of our observations on moderately conducting EuO near and below the Curie point. For less-conducting material well below the Curie point (20–40°K), and for all conductivity levels well above the Curie point ($T > 120^\circ\text{K}$), the λ^2 law is followed quite well. This will be taken up below.

For sample 66-2-10, a slope can be drawn through the α -vs- λ^2 data to give a best fit, though this is somewhat arbitrary. From these results, one needs to assume a value for the effective mass to obtain the variation of n_c/τ as a function of temperature. Since the conductivity is given by

$$\sigma = (e^2/m^*) n_c \tau \quad (3)$$

the scattering time and carrier density can be determined separately by measuring both α/λ^2 and σ . By combining (2) and (3), we can then obtain for the carrier density

$$n_c = m^* \left(\frac{4\pi^2 c^3 n \epsilon_0}{e^4} \right)^{1/2} \left[\sigma \left(\frac{\alpha}{\lambda^2} \right) \right]^{1/2}, \quad (4)$$

and for the scattering time

$$\tau = (4\pi^2 c^3 n \epsilon_0)^{-1/2} [\sigma (\lambda^2/\alpha)]^{1/2}. \quad (5)$$

Though this technique is far more cumbersome than a Hall-effect measurement, it does yield an experimental determination of n_c and τ . The results of this procedure carried out for sample 66-2-10 are plotted in Fig. 6. For these calculations the effective mass of EuO was chosen equal to the free-electron mass, i. e., $m^* = m_0$.

These results indicate that, in the temperature region near 50°K, a large decrease in the carrier concentration occurs as the temperature is increased. Below 50°K the electrons are degenerate and the scattering time changes little with tempera-

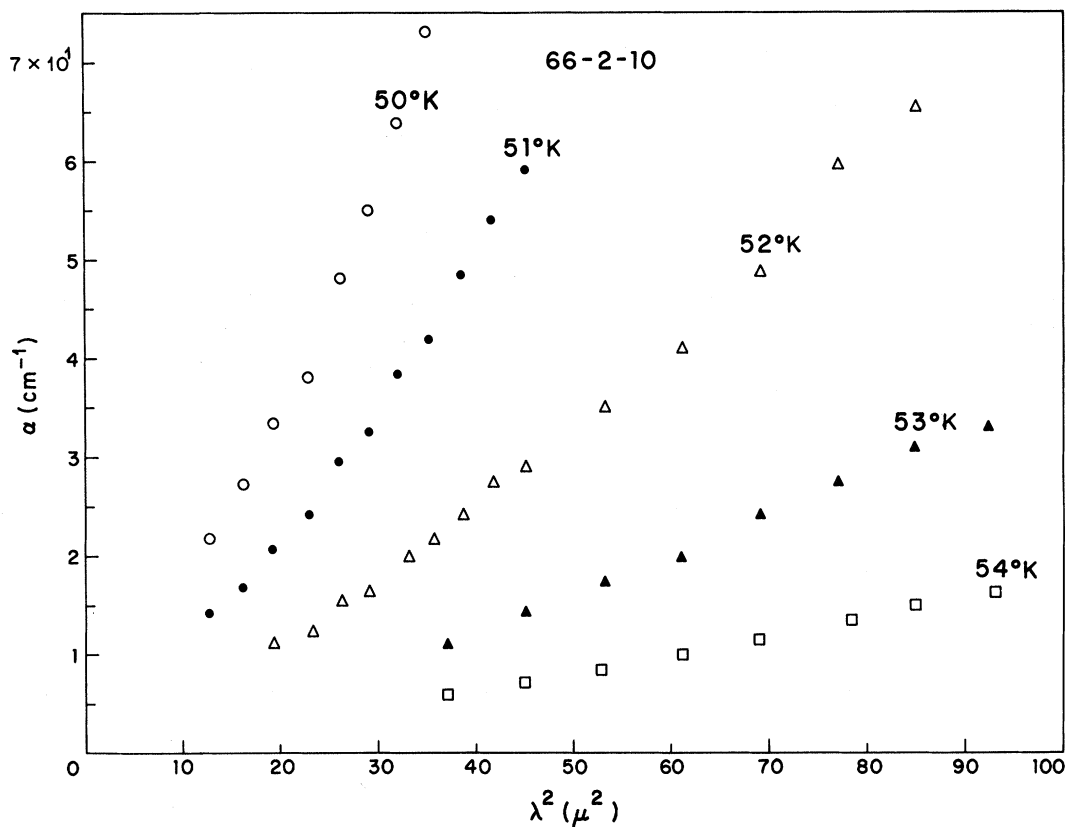


FIG. 5. Absorption coefficient α vs (wavelength)² for sample 66-2-10 as evaluated from the transmission curves of Fig. 3.

ture. This is reasonable, as changes in the magnetic disorder scattering should be small at temperatures 20°K removed from the Curie point. The mobility at 40°K, assuming $m^* = m_0$, is about 50 cm²/V sec. The large change in carrier concentration could account for most, if not all, of the observed change in resistivity in EuO for temperatures near 50°K.

C. Relations between Conductivity and Optical Absorption

Since the electrical behavior of magnetic semiconductors varies greatly with resistivity level, the optical absorption ascribed to free carriers was examined over a range of conductivities. This was done in order to correlate changes in resistivity behavior with optical-absorption behavior.

Turning to the behavior of $\alpha(\lambda)$, the absorption coefficient is plotted in Fig. 7 as a function of (wavelength)² for a lightly doped sample EuO 37 for temperatures $\leq 35^\circ\text{K}$. Its resistivity behavior is similar to that of sample 66-2-14 in Fig. 2. In this higher-resistivity sample, the absorption increases with decreasing temperature, and the λ^2 law is obeyed fairly well. At temperatures greater than 40°K no free-carrier absorption was detectable.

On the other hand, if a sample has sufficiently low resistivity, the free-carrier absorption can be observed for high temperatures. Experimental results are given in Fig. 8 for EuO 65, a low-resistivity sample whose electrical behavior is similar to that of sample 49-4 in Fig. 2. Curves are shown

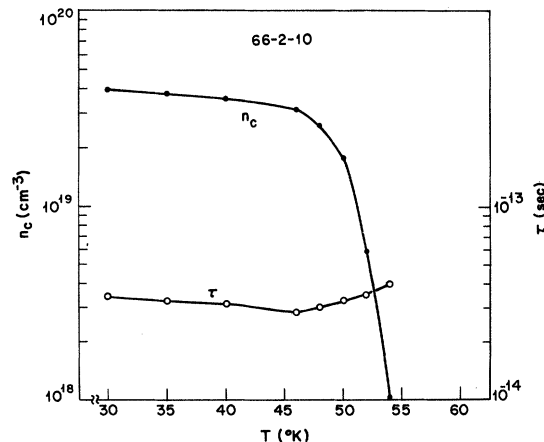


FIG. 6. Experimentally determined carrier density n_c and scattering time τ , as a function of temperature for sample 66-2-10.

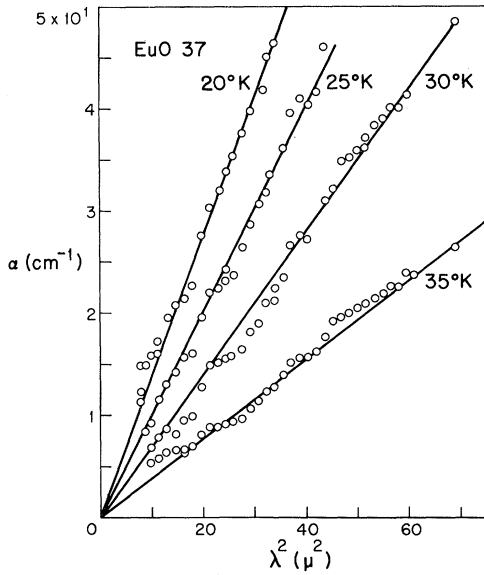


FIG. 7. Absorption coefficient α vs (wavelength)² for a lightly doped EuO sample at low temperatures.

for two temperatures well above the Curie point and, again, the absorption coefficient varies as λ^2 .

For moderately or heavily doped material at low temperatures (in the range of 120°K) the absorption increases more quickly than λ^2 , with a typical behavior being $\alpha \propto \lambda^{2.5}$ as in sample 66-2-10. The strongest dependence observed was $\lambda^{2.9}$ in highly conducting material. In material with lower resistivity than that of EuO 65, the absorption increases more quickly with wavelength than λ^2 , even at room temperature. Summarizing these observations, the absorption coefficient goes as λ^2 for low-conductivity material at all temperatures observable and for higher-conductivity material at high temperatures. The absorption exhibits a stronger λ dependence at low temperatures with increasing conductivity level. At sufficiently high conductivity levels, the absorption increase with wavelength is greater than λ^2 for all temperatures (at or below room temperature).

There is further relevant information that can be gleaned from the data presented above. The free-carrier absorption that is observed is continuous over the range of wavelengths from the optical-absorption edge out to 20 μ . There are no windows in transmission and the absorption monotonically increases with wavelength. The absorption has been quantitatively fit to a λ^2 law down to a wavelength of 2.3 μ . These observations imply that the conduction electrons exist in a band which is at least 0.5 eV wide. Even in the highest-resistivity material when the free-carrier absorption is observable, the absorption is continuous all the way up in energy to the optical-absorption edge. This argues

against conduction electrons existing in a narrow impurity band below the conduction band. Any mechanism proposed for conduction in EuO must place the electrons in a band at least 0.5 eV wide.

D. Temperature Variation of n_c and τ for Moderate-Conduction Samples

For moderately large electron concentrations, it is possible to observe free-carrier absorption throughout the entire temperature range. In sample 66-2-10, above 55°K the carrier concentration is too small to see free-carrier absorption. When a sample is sufficiently heavily doped so that the high-temperature carrier concentration gives a measurable free-carrier absorption, it is then possible to study both n_c and τ as functions of temperature over the entire temperature range. This procedure was carried out for three samples, 53V-10, 53V-12, and 62-1T-8. In all three cases the low-temperature absorption increased more quickly than λ^2 in the range of absorption coefficients observed. To determine n_c and τ from such data the absorption at some particular wavelength was somewhat arbitrarily selected. For these three samples, the wavelength chosen was between 3 and 4 μ . The results for sample 53V-10 are shown in Fig. 9. The resistivity ρ , the reciprocal carrier density $1/n_c$, and the reciprocal scattering time $1/\tau$ are all displayed as functions of temperature. The contributions of n_c and τ are determined by employing the free-carrier absorption results.

Several features of these results for 53V-10 are worth noting. The elbow in the resistivity curve at about 50°K is still present, even for this low-resistivity level. It is due primarily to variations in the carrier density. Between 48 and 60°K, the carrier density changes by almost a factor of 10, while the scattering time varies by less than a factor

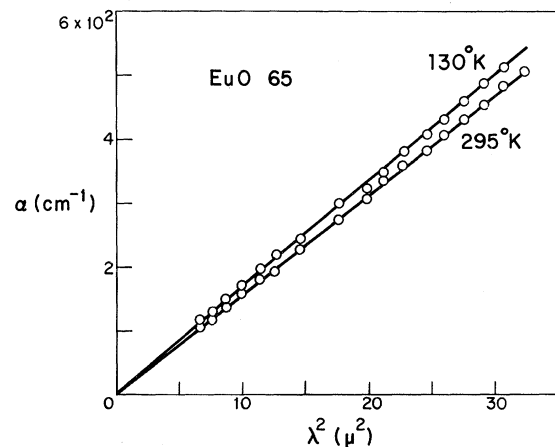


FIG. 8. Absorption coefficient α vs (wavelength)² for a moderately heavily doped sample at two temperatures well above the Curie point.

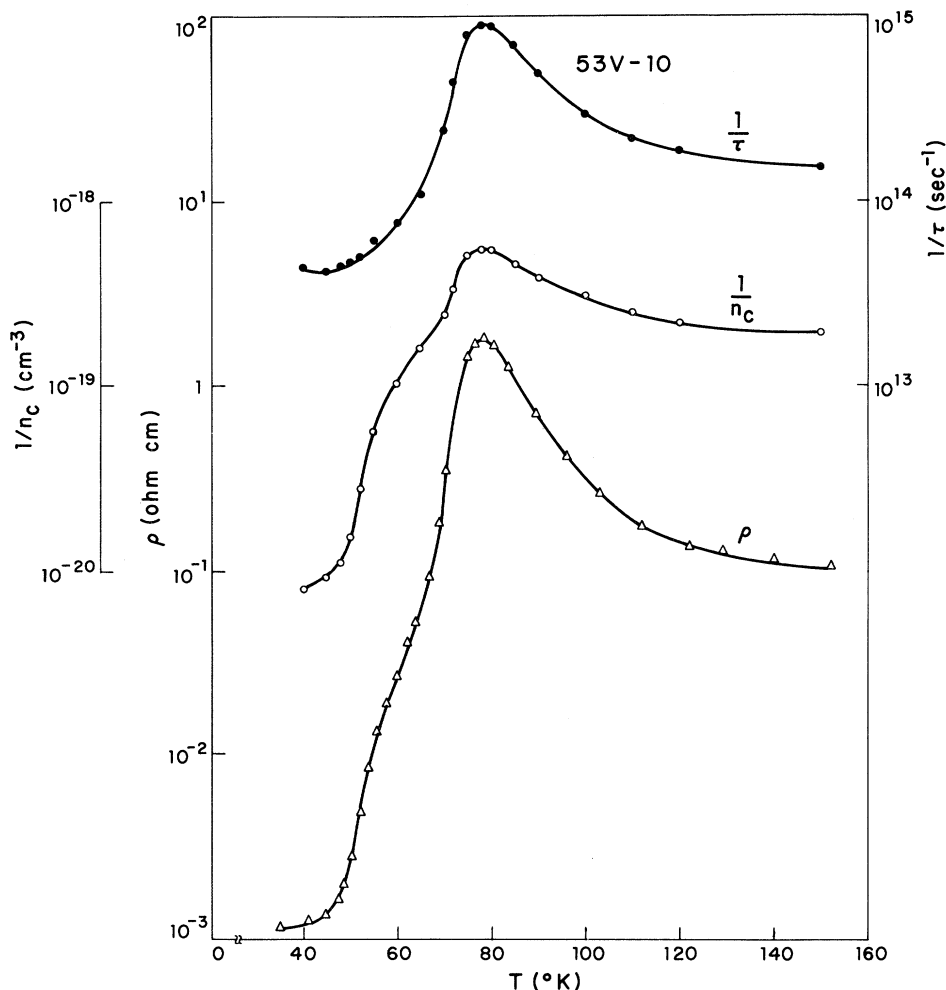


FIG. 9. Resistivity ρ , reciprocal carrier density $1/n_c$, and reciprocal scattering time $1/\tau$ as functions of temperature for sample 53V-10.

of 2. This behavior is similar to that observed in higher-resistivity material. In this relatively low-resistivity material, the structure near the Curie point is quite pronounced. The peak in resistivity between 75 and 80°K has contributions from both carrier-density changes and mobility changes. The major contribution is from variations in the scattering time τ , which changes about twice as much as the carrier density. The optical absorption, which depends on the ratio n_c/τ , is at a minimum between 60 and 65°K.

The variations of both n_c and τ near this peak are quite interesting. The carrier density drops around 70°K, reaches a minimum at the resistivity peak, and increases again. At about 150°K it approaches and passes its value at 65°K. The behavior of τ is also noteworthy. It exhibits some characteristics that have recently been proposed to explain the magnetic influence on the resistivity of nickel.⁷ The rate of change $d(\tau^{-1})/dT$ is greatest very close to the Curie temperature, as proposed, while the peak in $1/\tau$, and in the resistivity, occurs well

above the ferromagnetic Curie temperature. The peak is rounded, in contrast to the sharp peak predicted by the scattering theory of de Gennes and Friedel.⁶

In sample 53V-12 behavior similar to that of 53V-10 is observed. The results are shown in Fig. 10. The data plotted are of the same nature as in Fig. 9 for 53V-10. The resistivity level of 53V-12 is lower than that of 53V-10. By making a comparison between 53V-10 and 53V-12, it can be seen that the difference in resistivity between these two samples throughout the temperature range is largely due to changes in the carrier density and not scattering time. The result that changes in resistivity are a consequence of carrier-density changes is consistent with previously discussed results which, however, were limited to the temperature range below 55°K or so.

As the resistivity level is decreased, the contribution of the scattering time τ becomes more significant relative to that of carrier-density changes. In sample 53V-12, the scattering-time

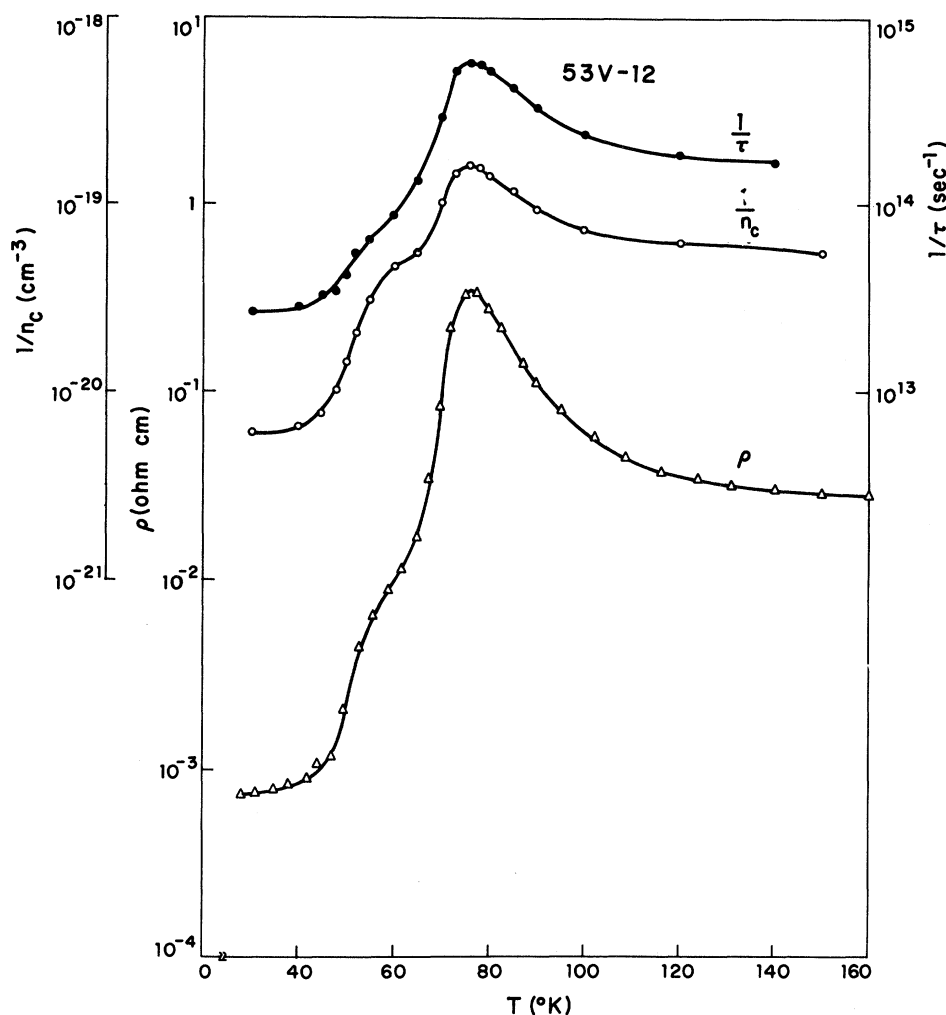


FIG. 10. Resistivity ρ , reciprocal carrier density $1/n_c$, and reciprocal scattering time $1/\tau$ as functions of temperature for sample 53V-12.

changes are about as large as the carrier-density changes though the variations occur at different temperatures. In both 53V-10 and 53V-12, the change in $1/\tau$ between 40 and 150°K is about a factor of 4. The $1/\tau$ variation with temperature is quite similar in both samples.

The peak in resistivity in 53V-12 is somewhat smaller than that of 53V-10. It is noteworthy that the peak is not shifted upward in temperature even though it is lessened in magnitude. As can be seen by comparing resistivity-vs-temperature curves for 62-1T-8 and 26-2 in Fig. 2, the peak in resistivity becomes smaller as it shifts upward in temperature. The results for 53V-12 show that the peak starts to diminish in size as a function of resistivity level before it starts to move to higher temperatures.

This comparison of optical-absorption results with resistivity data was also carried out on one sample with a shifted Curie point, sample 62-1T-8. The results for the third sample, 62-1T-8, are

presented in Fig. 11. The elbow at 50°K has disappeared. The carrier-density changes observed are far less pronounced than in sample 53V-12. The total change between 30 and 150°K is only about a factor of 3. The total variation in $1/\tau$ between these two temperatures is a factor of about 5. The situation is now the reverse of that at light doping levels. At these fairly large doping levels, enough to shift the Curie point, the mobility is rounded even further than in sample 53V-12. The $1/\tau$ contribution to the resistivity peak is still about twice that of the carrier density.

It was not possible to measure free-carrier absorption on more heavily doped material. The samples absorbed light too strongly, and only a small window in the transmission was observed just below the band edge in energy. However, the trends observed in the three samples shown in Figs. 9-11 show an interesting transition region. They illustrate the crossover from carrier-density-dominated behavior at light doping levels to

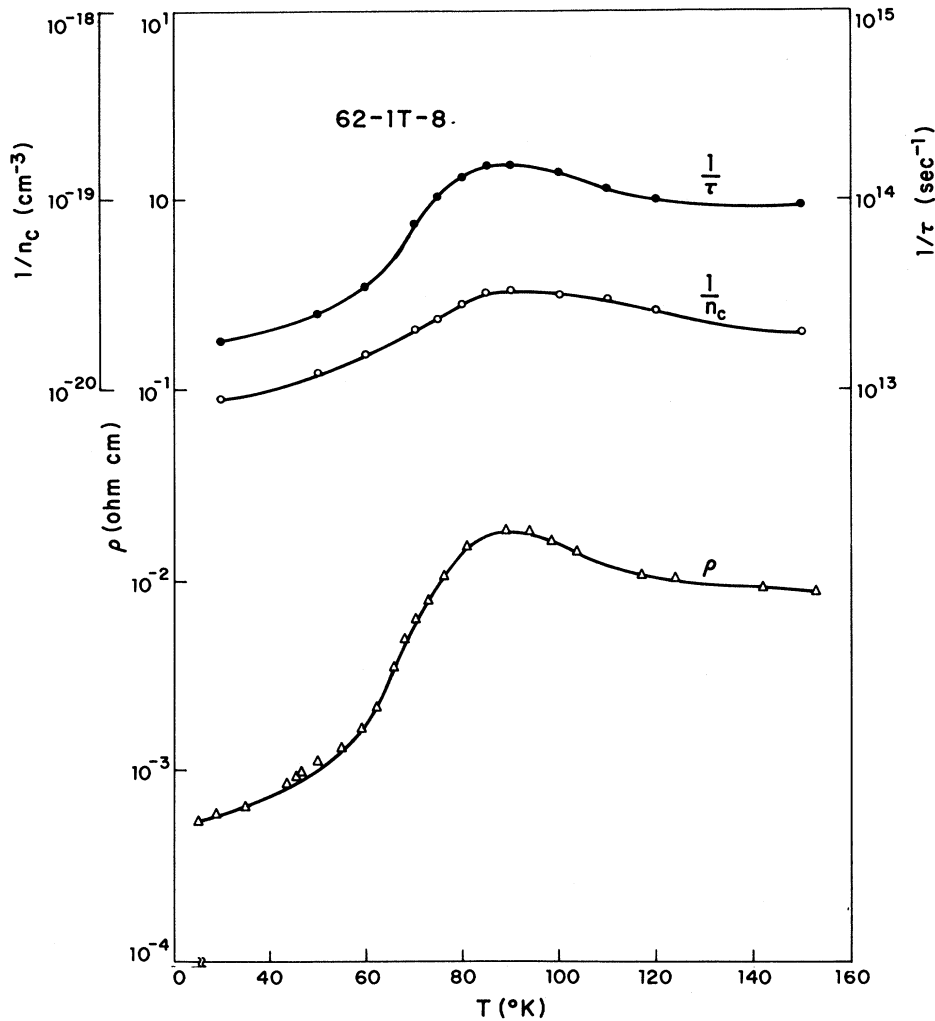


FIG. 11. Resistivity ρ , reciprocal carrier density $1/n_c$, and reciprocal scattering time $1/\tau$ as functions of temperature for sample 62-1T-8.

mobility-dominated behavior at heavier doping concentrations. This serves to connect some of our earlier reported results on the explanation of the elbow at 50°K with the work of von Molnar and Shafer¹⁶ on very heavily doped material with a shifted Curie point. They interpreted their results as due to spin-disorder scattering and this is consistent with the observations presented here. As the doping level is increased, the changes in carrier density decrease, and the mobility variations change in character, but remain roughly the same size.

From the results presented above the behavior of the conductivity of EuO as a function of temperature appears to be primarily determined by carrier-concentration variations at high- and moderate-resistivity levels. However, the resistivity peak between 75 and 80°K , observed in moderate-resistivity samples such as 66-6 and 49-4 in Fig. 2, has the same form as that in sample 53V-10, where it is determined to be primarily a mobility varia-

tion. It appears that the total ρ - T behavior for material with resistivity higher than that of 53V-10 is composed of a mobility term, which has a fixed form, more or less independent of resistivity level, and a carrier-density term. For samples with lower resistivity than 53V-10, the peak in $1/\tau$ decreases in magnitude with increasing conductivity level and sample 62-1T-8 has a much smaller peak than that of 53V-10. The ratio of high-to-low-temperature mobilities does not seem to decrease, however.

III. MODEL

The two features that accompany large-resistivity changes below the Curie point are the resistivity minimum at $\sim 15^\circ\text{K}$ in high-resistivity material and the elbow at 50°K in more moderate-resistivity material. Of these two features, the variety of behavior associated with the elbow has been the more extensively studied by the present authors. Assuming that the temperature dependence of the

mobility of 66-6 and 49-4 in Fig. 2 is the same as that of 53V-10, the carrier density of both these samples would remain relatively constant below 50°K. With increasing temperature, it would then drop sharply to a new value between 60 and 70°K and remain almost constant as the temperature is further increased. For sample 66-6 the carrier density increases with an activation energy at temperatures above 250°K.

The total change in carrier density from low temperatures (< 50°K) to high temperatures (> 100°K) decreases monotonically with decreasing resistivity level. As the low-temperature carrier-density level increases slowly, the high-temperature carrier-density level increases much more quickly, thus decreasing the total resistivity change between low and high temperatures.

In order to formulate a model of the electron-density change with temperature, the characteristics of the band of electron conduction were considered. Some authors have previously proposed conduction in a narrow impurity band, but optical-absorption experiments presented here have shown that conduction occurs in a band at least 0.5 eV wide, even at the lightest carrier concentrations measurable. The result that conduction is n type and occurs in a band at least 0.5 eV wide implies that conduction occurs in the lowest-energy conduction band. The optical transition that gives rise to the observed band edge is probably of the form $4f^7 - 4f^6 5d$, where the $4f$ electrons exist in highly localized states. Since the $4f$ electrons are so localized and have only small energy shifts ($\sim kT_c$) with the magnetic state of the crystal, the large observed shift of the absorption edge is due to the shift of the $5d$ states, which here are assumed to

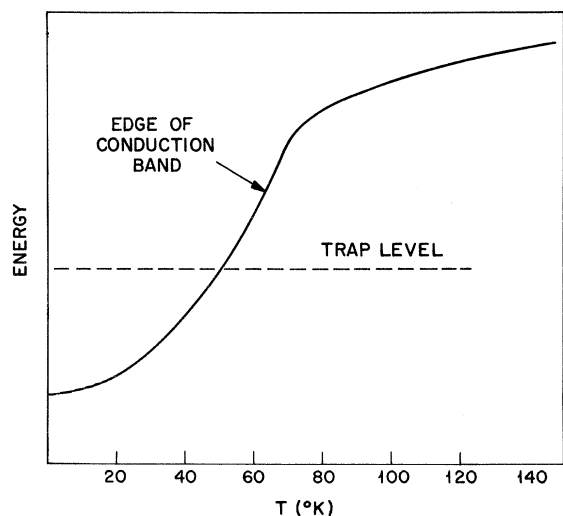


FIG. 12. Model for energy variation of conduction-band edge and trap level in EuO.

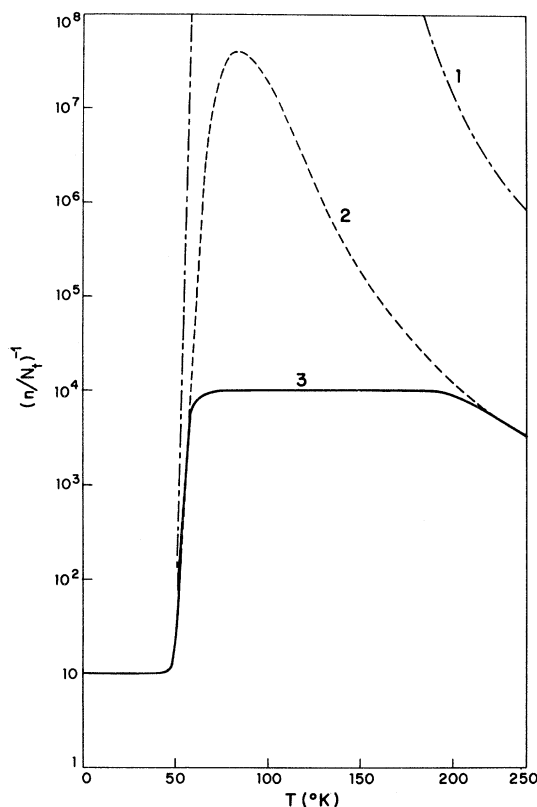


FIG. 13. Three normalized curves of reciprocal carrier density $(n_c/N_t)^{-1}$ vs temperature. For curve 1, $n < N_t$; for curve 2, $n = N_t$; and for curve 3, $n > N_t$, where n is the density of available electrons and N_t is the trap density.

form the lowest conduction band. Freiser *et al.*²¹ determined the total magnetic band-edge shift with decreasing temperature to be -0.26 eV.

The large change deduced in n_c , the carrier concentration in the conduction band, accompanied by the strong band-edge shift with temperature near and below the Curie point suggests the possibility of a level crossing the band edge. If a discrete temperature-independent level is placed in energy so as to cross the band edge near 50°K, the carrier variation can be determined for various values of trap-level density and available electron density. This simple model, illustrated schematically in Fig. 12, can account for much of the observed behavior in EuO. Lehmann⁵ has proposed a like model for n -CdCr₂Se₄.

In Fig. 13 are shown three types of behavior of $1/n_c$ that can be produced in this model for various ratios of electron density to trap-level density. In these curves the density of electrons available for conduction is given by n , the density of trap levels by N_t , and the effective spin-split conduction-band density of states by $N_c(T) = (2mm_0kT/\hbar^2)^{3/2}$.

Curve 1 is calculated with $n_c(40^\circ\text{K}) = n = 0.1N_t$.

Below 50°K the resistivity is independent of temperature, but at 50°K a sharp elbow is observed as the conduction electrons empty into the trap states. The quantity $1/n_c$ continues to rise above 50°K, since the only electrons in the conduction band are the thermally activated ones, with the Fermi level tied to the trap level. Similar behavior would be expected with n/N_t ratios up to almost unity. The resistivity is dominated by the exponential term and the peak will occur approximately at the temperature where

$$\frac{d}{dT} \frac{E_c(T) - E_F}{kT} = 0.$$

$E_c(T) - E_F$ is the difference in energy between the bottom of the conduction band and the Fermi level, which above 50°K is essentially tied to the trap level. From the optical experimental results on EuO, this situation should occur near 80°K. Well above the Curie point there is little band-edge shift with temperature, and the resistivity will exhibit an activation-energy behavior with the activation energy being roughly the energy difference between the conduction band and the trap level.

As the ratio n/N_t approaches unity, the temperature dependence of $1/n_c$ changes behavior. Curve 2 in Fig. 13 is plotted for $n/N_t = 1$. Above the peak, the activation energy is half that of curve 1, and, on a logarithmic scale, the peak is only half as large. Curve 2 represents a narrow transition region, as only a very small increase in the ratio n/N_t is required to produce the behavior of curve 3.

Curve 3 diagrams the situation for $n/N_t = 1.001$. The behavior below and near the elbow is similar to that of the other two curves, but when the traps become filled as the temperature increases above 50°K, the excess $n - N_t$ remains in the conduction band and the resistivity is flat as a function of temperature. Only when the temperature is sufficiently high to activate a number of electrons comparable to $n - N_t$ into the conduction band does the behavior of the $1/n_c$ curve change. The ratio of carrier densities above and below the 50°K elbow is just the ratio $(n - N_t)/n$. Thus small changes in the ratio n/N_t produce large variations in the total resistivity change across the elbow in this model.

The resistivity can be written as $(m^*/e^2)(1/n_c) \times (1/\tau)$ in order to emphasize that the changes in ρ are the product of changes in $1/n_c$ and $1/\tau$. The peak in resistivity near 75–80°K has nearly the same form and magnitude for all samples measured with resistivity level greater than that of sample 53V-10. For this sample, the major part of the variation is determined to be a $1/\tau$ variation (see Fig. 9). If a $1/\tau$ term having a temperature dependence similar to that of sample 53V-10 is assumed, the differences in resistivity behavior for

samples with resistivity higher than that of 53V-10 are qualitatively explained in terms of the model. The conclusions made from an examination of the experimental results and the model are that (i) a resistivity peak of fixed magnitude occurs between 75 and 80°K and is primarily a mobility change, and (ii) large changes of resistivity, due to carrier-density changes, can be accounted for through a trap level crossing the conduction band.

An unusual feature of this model is the relationship of the trap-level density to the total electron density. The experimental results, over a fairly wide range of resistivities, are explained in terms of the model if the two quantities are assumed to be almost equal. Whatever mechanism contributes a trap-level state appears also to contribute an electron. Several factors related to the growth of the crystals suggest an oxygen vacancy as the trap level, as will be discussed. A similar explanation has been proposed by Amith and Gunsalus²² to account for the electrical properties of the chalcogenide spinels. The oxygen vacancy would be able to capture two electrons, the first being very tightly bound, and the second not so tightly bound. Presumably then, in EuO, the oxygen vacancy would at most be singly ionized.

It was mentioned earlier that type-A behavior is associated with growth using starting materials

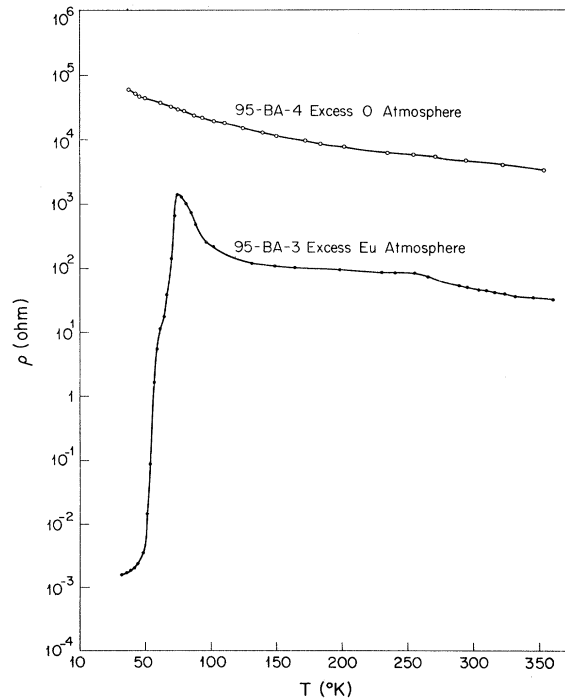


FIG. 14. Resistivity vs temperature for two annealed EuO samples. The upper curve is for a sample annealed in an excess-oxygen atmosphere and the lower curve for a sample annealed in an excess-europium atmosphere.

having an excess amount of Eu above stoichiometry. This situation is consistent with the attribution of the trap to an oxygen vacancy. As a further test of this proposal, an annealing run was made on some insulating ($> 10^8 \Omega \text{ cm}$) material. Two samples were annealed at 1400°C for several days. One sample was annealed in an atmosphere equilibrated on the Eu-rich side of stoichiometry, while the other was annealed in an oxygen-rich atmosphere. Though the starting material had resistivity too high to measure, that of both annealed samples was measurable. The temperature dependence of the resistivity for both samples is shown in Fig. 14. That of the oxygen annealed sample is similar to type-B behavior while the sample annealed in excess Eu has type-A behavior, exhibiting the sharp elbow at 50°K and the large-resistivity rise above it. The introduction of conduction electrons, and an almost equal number of trap levels, thus appears to be a consequence of an excess of europium whether produced in growth or by annealing.

The small deviations from the 1:1 ratio of electrons to traps can be accounted for, and even expected, in actual crystals. First, there will be some compensating defects such as Eu vacancies. There will also be residual impurities such as other rare earths. Also, second-order effects due to two oxygen vacancies being nearest neighbors might create two levels, one higher and one lower than the two original levels. If the upper level is above the conduction-band edge at all temperatures, there would be an excess of electrons over available trap states. The relative influence of each of these possible effects should vary from crystal to crystal.

When the tentative identification of the oxygen vacancy with the trap level was first made, the oxygen vacancy was assumed to be quite localized. This was considered necessary so that exchange effects with the neighboring europium atoms would be small. If these effects were not small, then the level would drop in energy with increasing magnetization, and the electronic repopulation as a function of temperature would not be as dramatic.

In applying the model of Fig. 12 to EuO , to determine if a quantitative fit to experimental results was possible, a total relative band-edge-to-trap-energy shift of 0.26 eV, as reported by Freiser *et al.*,²¹ was used. Quantitative fits to the curves, however, could not be obtained with this value. A total shift of about 0.45 eV is necessary to reproduce the observed experimental behavior.

This discrepancy may have several possible explanations. In the paper by Freiser *et al.*,²¹ there appear experimental results which indicate a total shift of about 0.35 eV. In addition, there is some conflict with the reflectivity results of Feinleib *et al.*,²³ whose data show that the lowest-energy

peak shift with temperature may correspond to a total band-edge shift with temperature of about 0.5 eV. In light of this conflicting evidence, it is quite possible that the total band-edge shift could actually be around 0.45 eV.

A. Magnetic Double Donor

Even if the band-edge shift should turn out to be less than 0.45 eV, a more refined model for the energy levels of the oxygen vacancy that we shall now describe may completely resolve the problem. A similar model has been independently proposed by von Molnar.²⁴ The model should be generally valid for any double donor in a ferromagnetic crystal.

Consider the case where the wave functions of both electron states are sufficiently delocalized that there is some exchange interaction with the neighboring Eu^{++} spins. First, we look at the singly ionized oxygen vacancy. At high temperatures ($T \gg T_c$) there is no spin alignment of the captured electron since there is no magnetic order (neither short nor long range) and no exchange energy can be gained. As the temperature is lowered below the Curie point, the captured electron becomes aligned (say, spin down) and its energy decreases.

Next consider the case where the vacancy is occupied by two electrons. The spins of the electrons will be paired in this situation and there will be no magnetic moment. This means that the total energy of the two-electron state will be independent of magnetic influences and to first order will not shift when the crystal becomes magnetized.

When the crystal is fully magnetized, the energy of this two-electron state is nearly the same as when the crystal is entirely demagnetized. Now consider the energy of the two-electron state composed of one electron in the spin-down conduction band and one electron in the spin-down trap level. When the crystal is fully magnetized, the energy of this two-electron state is decreased by $E_0 + E_1$. Here E_0 is the total magnetic shift of the spin-down conduction band. E_1 is the downward shift in energy of the spin-down trap level, and is probably equal to or less than the total shift of the conduction band E_0 . If we define α by setting $E_1 = \alpha E_0$, then the total decrease in energy of the two-electron state composed of a spin-down conduction-band electron and a spin-down trapped electron is then $E_T = (1 + \alpha)E_0$, which is equal to or greater than the total conduction-band shift. There are four combinations of an electron in a spin-up or spin-down conduction band and in a spin-up or spin-down trap level. We have discussed above only the lowest-energy states of the four combinations. The lowest-energy state varies qualitatively with temperature as does the conduction-band edge, but the total shift is greater by a factor of $1 + \alpha$.

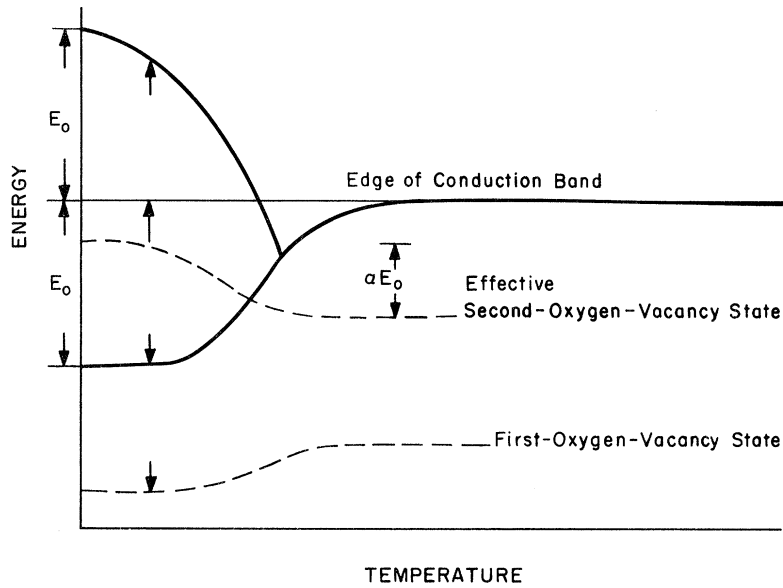


FIG. 15. Energy-level-vs-temperature diagram for EuO. Spin-up and spin-down trap-level states are shown as well as spin-up and spin-down conduction bands.

The two-electron energy-level scheme just described can be interpreted in terms of an effective one-electron energy-level diagram. This is done in Fig. 15. The lower level is that of *one* electron at the trap site with its spin aligned with that of the crystal. The second level shown is an effective one-electron level for the second electron at the trap site. Because it has to have its spin paired with that of the first electron, it has its spin in the opposite direction to that of the crystal. The two trap levels shown in Fig. 15 are for the lowest-energy states for the first and second electrons added to the double-donor site. The conduction-band behavior shown is similar to that described by Baltensperger.²⁵

Another way of looking at this problem is to consider the spin of the second electron. When it is in the conduction band, it can go into the lower-energy band, the spin-down band. On the trap level, however, the only state unoccupied is a spin-up state. With increasing magnetization, the band is lowered in energy, and the trap state is raised in energy.

The unusual feature of the donor-level energy increasing with increasing magnetization is a direct consequence of the level in question being the second level of the vacancy, the first already being occupied with a spin-down electron. This result makes the total energy shift of the conduction-band edge required for quantitative agreement of the model with experiment somewhat smaller. A shift of 0.45 eV would duplicate the experiment closely in terms of the model first proposed. By incorporating the magnetic-double-donor model with $\alpha = 0.5$, a shift of 0.30 eV would produce similar results. The observed electrical behavior can be well re-

produced in the model by selecting an α and E_0 so that

$$(1 + \alpha) E_0 \approx 0.45 \text{ eV} .$$

An accurate experimental determination of E_0 would thus give some measure of α and the delocalization of the electrons at the oxygen vacancy site.

B. Mobility

The temperature variation of $1/\tau$ for samples 53V-10, 53V-12, and 62-1T-8 (shown in Figs. 9-11) is similar to that of magnetic-scattering models of several authors. The high-temperature (here, 150°K) values of τ for all three samples are around 10^{-14} sec. Using $m^* = m_0$, this gives mobilities within a factor of 2 of the $10\text{-cm}^2/\text{V sec}$ value reported by others.

For very low temperatures, τ is around 5×10^{-14} sec in all three samples. According to several authors⁶⁻⁸ employing various theoretical approaches, the low-temperature behavior of τ is given by $1/\tau \propto 1 - J^2$, where $J = M/M_0$ and M_0 is the saturation magnetization. The experimental results show that τ appears to level off below about 50°K in all three samples. This suggests that another scattering mechanism becomes dominant in this temperature regime. According to all the authors, the high-temperature magnetic scattering is from a completely disordered spin lattice, and they arrive at equivalent results.

Near the Curie point, the predictions⁶⁻⁸ for τ disagree, and it is here that our experimental results are most interesting. Experimentally the mobility peak is rounded, and occurs well above the Curie point. As can be seen by comparing the resistivity curve and the $1/\tau$ and $1/n_c$ curves for the three

samples, a small variation occurs in the carrier concentration which closely follows the $1/\tau$ variation. This change of n_c above the Curie point may be only apparent because inaccuracies in the method of analysis or of some consideration not yet taken into account.

Though it is not obvious from the presented data, the magnitude of the peak in $1/\tau$ relative to a higher-temperature value (say, 150°K), changes very little for samples with resistivity higher than that of 53V-10. The temperature position of the peak does not change either. As the sample resistivity level decreases from that of 53V-10, the magnitude of the peak decreases also. This is evident in Figs. 9-11. For the lowest-resistivity samples measured, such as 26-2 in Fig. 2, the increase in resistivity at the peak is only about 20%.

The fact that the maximum occurs above the Curie point implies the existence of short-range interactions, since theoretically⁶ the peak should occur exactly at the Curie point if there are only interactions with the long-range magnetic order. Major differences between the results presented here and the predictions of Fisher and Langer⁸ include the fact that the magnitude of the peak does not increase with decreasing doping for resistivities above those of sample 53V-10. Neither does the peak move any closer to the ferromagnetic Curie point with decreasing doping as predicted.

IV. FURTHER EXPERIMENTAL RESULTS AND INTERPRETATIONS

A. Low-Temperature Minimum

Another characteristic which we attribute to carrier-density changes in EuO is the minimum in the resistivity which occurs at around 15°K . As mentioned earlier this type of behavior has been reported by von Molnar,¹⁸ and he explains his results in terms of impurity-band hopping.

We have also studied this behavior and have noted several characteristics which have led us to propose an alternative model for this phenomenon. To see the motivation for this proposal, the low-temperature resistivity of 34-2-30 is plotted versus $1/T$ in Fig. 16. Below the minimum the resistivity increases, and the increase follows an activation energy. The activation energy (the slope of the dotted line) is 18.3 meV.

This behavior could correspond to activation from a simple hydrogenic impurity (e.g., in EuO, a normally trivalent rare earth such as Gd or La) in EuO. This is in no way related to the band crossing a oxygen-vacancy magnetic-double-donor trap level as described above, but is quite similar to behavior observed in normal semiconductors, e.g., GaAs. If one assumes a simple hydrogenic model, and uses Axe's²⁸ value of 23.9 for the dielectric constant, an effective mass of $0.77m_0$ is

required to fit the results shown in Fig. 16.

This is in reasonable agreement with an effective mass estimated by comparing room-temperature Hall effect, free-carrier absorption, and resistivity for one sample (62-1T-8). This measurement yielded $m^* = (1.0 \pm 0.2)m_0$. Several other authors have estimated the effective mass, and the most recent work is that of Phipps²⁷ who employs reflectivity results and obtains $m^* = 0.95m_0$.

Good agreement can be obtained between the hydrogenic impurity model and experiment for the resistivity decrease with increasing temperature ($T < 15^\circ\text{K}$), but this does not account for the occurrence of the minimum in the ρ -vs- $1/T$ curve and the increase in resistivity ($T > 15^\circ\text{K}$) with increasing temperature. A possible explanation for this minimum may be as follows. With increasing temperature the conduction-band minimum is presumed to move upward in energy. If the initial state of the optical transition is assumed constant in energy, as discussed above, this is consistent with experimental observations. It also agrees with the theoretical result of Haas⁷ who states that, to first order, the magnetic shift of the band edge is given by

$$\Delta E = E_0(M/M_0),$$

where M_0 is the saturation magnetization. In this first approximation the band edge varies as the long-range order, or the magnetization, because the conduction-band states are states of the entire crystal. On the other hand, the electron bound to the hydrogenic impurity is essentially localized to within the Bohr radius of the impurity. The short-range order within the Bohr radius is the "magnetization" that the bound electron sees, and this decreases less quickly with increasing temperature

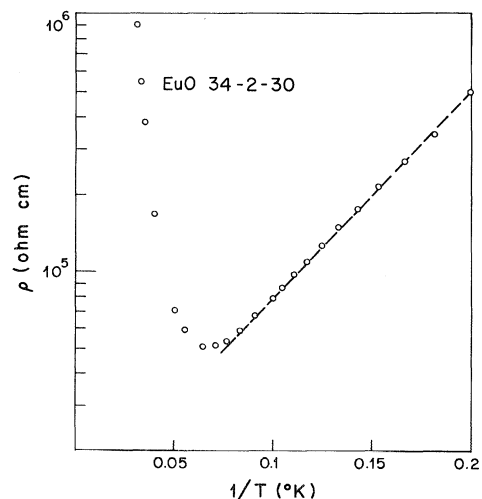


FIG. 16. Resistivity vs reciprocal temperature for sample 34-2-30.

than the long-range order. This leads to a greater exchange energy for the bound electron relative to an electron in the conduction band. This approach does not require invocation of the concept of "self-trapping,"⁹ nor is it necessary for any additional magnetic ordering to occur near the impurity site in order to have a difference between long- and short-range order.

Since the magnitude of the exchange energy of the bound electron decreases less quickly than that of an electron in the conduction band, the energy separation between the bottom of the conduction band and the bound electron increases with increasing temperature for $T < T_C$. For $T > T_C$, however, the first-order magnetic contribution to the energy of the conduction-band states is zero, and that of the bound electron decreases with increasing temperature, so the energy separation between the impurity level and the conduction-band edge decreases with increasing temperature. The binding energy of the impurity state should be the same at high temperatures (i. e., $T > 150^\circ\text{K}$) as it is at low temperatures ($T < 15^\circ\text{K}$), assuming that the effective mass has not changed.

At sufficient concentrations of residual impurities such as rare earths like La or Gd, these impurity states will overlap and begin to merge with the conduction band. This effect would be expected to diminish the activation-energy behavior, and less freezeout should occur below the minimum. This behavior is observed in normal semiconductors such as GaAs where the doping is sufficiently great to cause overlap of impurity wave functions. Again, this proposal concerning the minimum at 15°K is not related to the magnetic-double-donor concept discussed above.

When the density of oxygen vacancies becomes significant, they will contribute electrons below 50°K , with no impurity states below the band edge. Their presence will further wash out the minimum at 15°K . This is seen in Fig. 2, sample 66-2-14, where the minimum is much shallower than in 34-2-30. The pattern of behavior goes from the existence of the minimum at 15°K in high-resistivity samples to that of the elbow at 50°K in moderate-resistivity samples.

B. Magnetoresistance

Negative-magnetoresistance effects were first observed in ferromagnetic semiconductors in 1967. von Molnar and Methfessel⁴ reported a giant negative magnetoresistance in Gd-doped EuSe and Haas *et al.*²⁸ reported negative magnetoresistance in CdCr_2Se_4 . von Molnar and Methfessel attributed the resistivity to a hopping mechanism and the resistivity peak near the Curie point to a trapping of electrons in polarized spin clusters, in which an applied magnetic field decreases the spin disorder

and allows more hopping. Haas *et al.* compared their observations to a critical-scattering model in which the observed resistivity variations are all due to mobility changes. Again, an applied magnetic field would decrease the spin disorder near the Curie point and increase the mobility.

Here, and in earlier work, we have shown that the resistivity changes in our EuO crystals appear to be primarily carrier-density changes except for the peak just above the Curie point which is mostly a mobility effect. Fortunately, the elbow at 50°K observed in moderately doped samples is well removed in temperature from the peak between 75 and 80°K , which allows the resistivity variations associated with each feature to be more easily distinguished from one another than would be the case if the elbow occurred at, say, 65°K . One similar resistivity curve has previously been presented for EuO.¹⁹ In Fig. 17 are shown the ρ -vs- T curves for various applied magnetic fields for sample 66-2-24 which is $480\ \mu$ thick.

The curves have several distinctive features. At low magnetic fields there is no significant change in the structure of the elbow at 50°K . At a 16-kG applied field it is shifted upward about 2°K . In terms of the model, this means that the temperature at which the conduction band crosses the trap level has increased. For a 48-kG applied field the

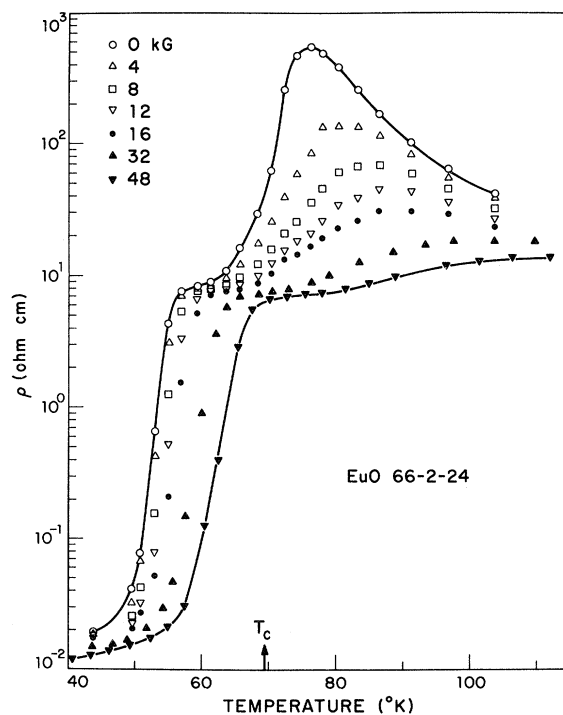


FIG. 17. Resistivity vs temperature for sample 66-2-24 at several values of applied magnetic field, showing large negative magnetoresistance.

elbow is shifted upward about 10°K, and at these fields $d\rho/dT$ is smaller above the elbow than for the zero-field case.

This elbow shift is expected as a result of the model. The energy of the absorption edge, associated with the conduction-band minimum, increases less quickly with temperature under applied magnetic field. Hence, one expects the conduction band to cross the trap level at a higher temperature in the presence of a magnetic field. It is difficult to make quantitative comparisons between the model and the electrical results for this temperature regime, as the optical-absorption edge has not been thoroughly investigated as a function of temperature and magnetic field. However, the physical behavior expected from the model in order to get agreement with experiment is reasonable; it is not necessary to postulate any extraordinary band-edge shift with magnetic field.

An interesting feature of these resistivity curves is the occurrence of a shoulder at the same resistivity level independent of magnetic field. This is expected from the model. When the band edge is well above the trap level in energy, the traps are effectively all filled. The number of electrons in the conduction band does not decrease further with increasing temperature, as there are no more trap levels to be filled. The application of a magnetic field increases the temperature at which the trap levels become filled but the number of excess electrons remains the same. The resistivity shoulder should therefore remain at the same level, as is observed.

Under relatively small fields the peak near 76°K is decreased and displaced to higher temperatures. A 4-kG field, which has little effect on the elbow at 50°K, reduces the maximum resistivity at the peak by a factor of 4. Since the resistivity changes associated with the peak occur over a much wider temperature range, the difference in behavior between the elbow and the peak becomes even more pronounced.

These differences can be emphasized by considering the normalized resistivity for various magnetic fields as a function of temperature. This is done in Fig. 18 where $\rho(B)/\rho(0)$ is plotted as a function of temperature for four applied magnetic fields. The separation of the two phenomena is more apparent in this figure. The resistivity changes associated with the elbow only occur between about 50 and 60°K. Magnetic field effects associated with the mobility peak become important several degrees below the Curie point. For the fields shown, the 4-kG curve has a much larger change for the mobility peak region than for the 50°K elbow region. As the field is increased, however, the differential change associated with the elbow stays about the same, while that associated

with the mobility peak strongly decreases. This is consistent with the resistivity increase above the shoulder at ~60°K being attributed to critical magnetic scattering. The total contribution that magnetic scattering can make is only the difference in resistivities between the shoulder and the peak.

Some qualitative magneto-optical-absorption measurements were made on another sample that exhibited free-carrier absorption for all temperatures. At temperatures near the elbow at 50°K, when a magnetic field was applied, the free-carrier absorption increased. Since the resistivity decreases with applied field at these temperatures, this means that the major part of the resistivity change near 50°K is due to carrier-density changes, which is consistent with our previous assignment. Similarly, when a magnetic field was applied with the sample at ~80°K, the free-carrier absorption decreased. Since the resistivity decreases with applied magnetic field, we conclude that the major part of the resistivity change is due to mobility variations with magnetic field in this temperature region. Again, this confirms our earlier description.

The curves of resistivity under applied field for samples of different resistivity levels also agree with the predictions of the trap-level model and the attribution of the peak at 76°K to a mobility change. Results for a sample with considerably larger resistivity, 66-6, are shown in Fig. 19. In this sample, the total resistivity change is much larger than

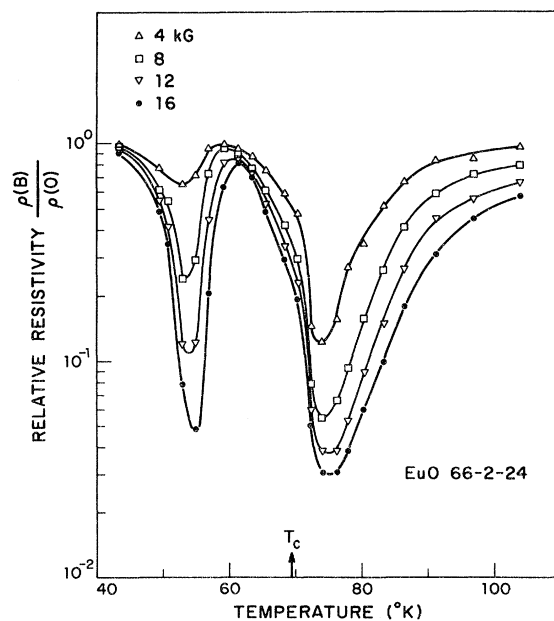


FIG. 18. Normalized resistivity vs temperature for small applied magnetic fields for sample 66-2-24. The separation of the two effects near 50 and 76°K is emphasized.

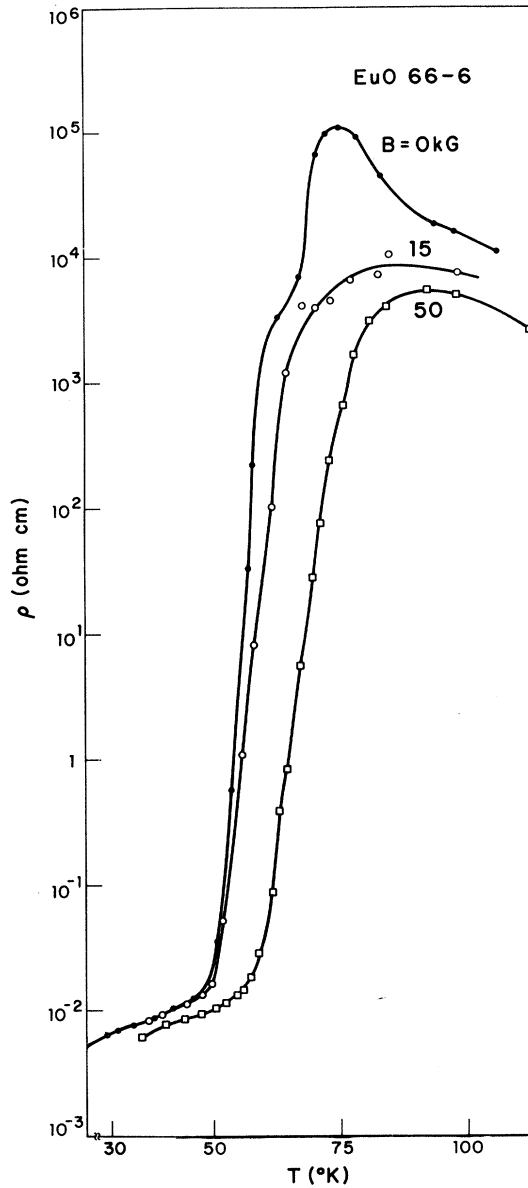


FIG. 19. Resistivity vs temperature for a higher-resistivity sample 66-6 for three magnetic fields (0, 15, 50 kG).

in sample 66-2-24 in the temperature range $50^\circ\text{K} < T < 70^\circ\text{K}$. The difference is expected to be due to larger carrier-density changes, and not larger mobility changes. As can be seen, the results are consistent with this expectation. A 15-kG field essentially flattens out the mobility peak, but only changes the position of the elbow a couple of degrees. This behavior is similar to that of sample 66-2-24. The slope $d\rho/dT$ above the elbow is somewhat decreased. For the 50-kG curve, the elbow is shifted almost 10°K and $d\rho/dT$ above the elbow is much smaller than in the zero-field case. Magneto-optical-absorption measurements indicate

that the band edge is lowered in an applied field, and for a given field the greatest effect is observed near the Curie point. For temperatures below the Curie point, then, the rate of change in energy separation between the trap level and the band edge with temperature will be decreased, resulting in a lower $d\rho/dT$ in terms of the model.

The series of results presented here is quite different from those previously presented in the literature.^{4,7} The behavior exhibited is consistent with the large resistivity change associated with the elbow at 50°K as being due to carrier-density changes and the peak at 80°K as due to a mobility variation. Their relative magnitudes as functions of doping also agree with these identifications.

C. Pressure Effects

To test various aspects of the proposed model for

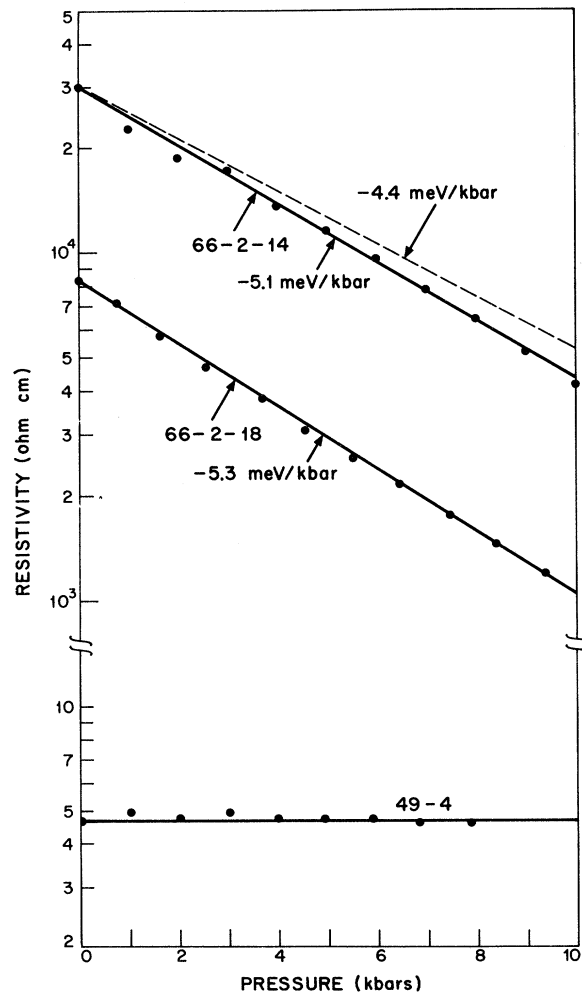


FIG. 20. Room-temperature pressure variation of resistivity of three EuO samples. The dashed -4.4-meV/kbar line is the expected behavior from the model using Wachter's results (Ref. 27) for dE_g/dP .

conduction in EuO, the pressure dependence of the electrical resistivity of EuO at room temperature was also measured. This work has been reported earlier,¹⁵ but will be summarized here for completeness.

The room-temperature resistivity pressure measurements were made on a variety of crystals and the results for three representative samples are shown in Fig. 20. The ρ - T curves for these samples can be seen in Figs. 1 and 2. For sample 49-4, the lowest-resistivity sample, the resistivity is independent of pressure. For the highest-resistivity samples 66-2-14 and 66-2-18 the pressure coefficient is given by

$$\frac{d \ln \rho}{dP} \approx 0.20 \text{ kbar}^{-1} .$$

If this variation is interpreted in terms of a pressure-sensitive electrical activation energy, we obtain

$$kT \frac{d \ln \rho}{dP} \approx -5.2 \text{ meV/kbar} .$$

This is quite close to the observed shift of the room-temperature optical-absorption edge of -4.4 meV/kbar as reported by Wachter.²⁹

By comparing the ρ -vs- T and ρ -vs- P curves for all three samples, a connection is apparent. Where the resistivity exhibits high-temperature activation-energy behavior, it exhibits a pressure variation of resistivity. When the resistivity varies slowly with temperature as in 49-4, it is also pressure independent. The two highest-resistivity cases correspond to the case of fewer electrons than traps, while the lowest-resistivity case corresponds to the situation of more electrons than trap levels.

As stated above the pressure-dependent activation energy of -5.2 meV/kbar is quite close to that of the shift of the optical-absorption edge, -4.4 meV/kbar. By using a -4.4 -meV/kbar variation instead of a value of -5.2 meV/kbar, only a 20% departure from the experimental results would occur at a pressure of 10 kbar. These results are consistent with a model in which conduction occurs in a band whose energy varies with pressure as does the observed optical-absorption edge, and a trap level whose energy is constant.

The qualitative predictions of the model in regard to the pressure variation, however, do not depend on the precise positions of energy levels. Pressure variation of the resistivity should occur when there are fewer electrons than traps (high-resistivity samples), as any relative change between the trap level and the conduction-band edge will change the number of carriers in the conduction band. For the case of more carriers than traps, the resistivity should be pressure independent until such pressures are reached where the number of activated

carriers becomes comparable to the number of carriers already in the band ($n - N_t$). As a function of temperature and at zero pressure, the former case should exhibit an activation-energy behavior and the latter should be temperature independent. As can be seen from Figs. 1, 2, and 20, all these correlations are observed.

D. Low-Resistivity Behavior

The lower-resistivity doped samples of EuO exhibit transition behavior. The peak moves upward in temperature and the elbow at 50°K disappears. In order to observe this transition behavior in more detail than can be obtained from examining Fig. 2, several resistivity curves for higher-conductivity samples are shown in Fig. 21. A curve similar to that of 26-2 has been published by von Molnar.¹⁶ These curves overlap somewhat and do not exhibit such a nice pattern as those of Fig. 2. The effect of the Curie-point shift with increased conductivity first reported by Holtzberg *et al.*³⁰ is apparent in sample 82-0-5 and those with lower resistivities. The elbow at 50°K is only present in the curves whose Curie points have not shifted. As mentioned earlier, the peak in resistivity of 53V-12 is small-

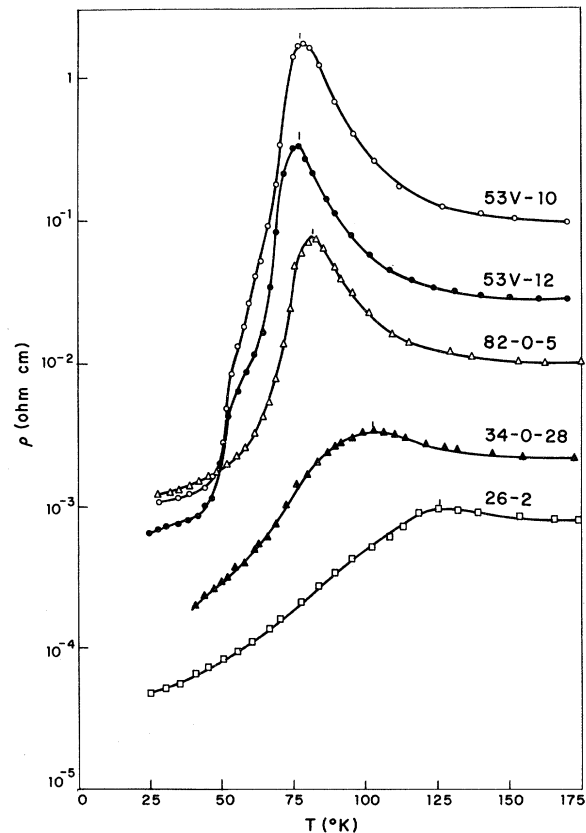


FIG. 21. Resistivity vs temperature for lower-resistivity EuO samples.

er than that of 53V-10, indicating the peak starts to decrease in magnitude before it shifts upward in temperature. The peak continues to decrease in magnitude with decreasing resistivity level.

In summary, several general trends can be noted from these curves. The first is a decrease of the effects of carrier-density changes. Since the electrons are presumed to be mostly from dopant donors (La or Gd) in high-conductivity samples, and not from oxygen vacancies, no trap levels would be added by their presence, thus minimizing the effects of carrier-density change. Second, the peak due to spin-disorder scattering continuously decreases with increasing conductivity. A third effect is the Curie-point shift with increased doping.

V. CONCLUSIONS

Many of the electrical studies on ferromagnetic semiconductors have been hampered by the difficulty of separating contributions to the conductivity of carrier density and scattering time. Hall-effect measurements near the Curie point of such materials have not yet been made. Due to the low mobility and large magnetoresistance of these materials, the application of a magnetic field causes a large change in resistance which masks any small Hall effect that might exist.

In taking another tack, optical measurements on conducting samples have shown the existence of free-carrier absorption. The nature of the absorption indicates that the conduction electrons are in a band at least 0.5 eV wide. When the free-carrier-absorption results are compared with the conductivity results, both the carrier density and scattering time can be experimentally determined. This procedure only works when n_c/τ is sufficiently large so that free-carrier absorption can be measured, but it has enabled us to determine that the large changes in resistivity associated with the elbow at 50°K are primarily carrier-density changes, and not mobility changes. We have also found that the peak in resistivity that occurs above the Curie point is mostly a mobility effect. There may also be a small carrier-density change that follows the mobility change, which may be real or may be only apparent because of some consideration not yet taken into account. The mobility on the high-temperature side of the peak is a factor of 3-4 smaller than that on the low-temperature side.

For sufficient carrier concentrations, the Curie temperature of EuO increases and the size of the mobility peak decreases. Both of these effects appear to be continuous functions of doping and have been observed previously in EuO and the other Eu chalcogenides. The band of electron conduction is assumed to be the final state of the optical-absorption edge. The temperature variation of the edge is felt to be due to the variation of the final state

of the transition as the initial state is the $4f^7$ configuration, which is quite localized and should only be perturbed by energies of the order of kT_c .

A model consisting of a conduction-band edge varying in temperature as the final state of the optical-absorption edge and a fixed-energy trap level crossing the band at 50°K was proposed. The model produces resistivity curves that are quite similar to those experimentally observed when the number of traps and the total number of electrons are almost equal. Small variations around unity in the ratio of electrons to traps produce large changes in behavior, again quite similar to experimental results.

The trap level has been tentatively identified as an oxygen vacancy by comparison with growth procedures. Further consideration of the character of electron states associated with an oxygen vacancy leads to the idea of the magnetic double donor. One of the difficulties with the fixed-energy trap level was that it was necessary to postulate a high degree of localization in order for the level to be relatively independent of magnetic effects. In the ground state of magnetic double donor the electron spins are paired resulting in magnetization-independent energy.

The low-temperature minimum observed in the resistivity of EuO around 15°K has been ascribed by other authors to an impurity-hopping mechanism. An alternative proposal is presented here which is based on activation of carriers from a rare-earth impurity into the conduction band. This proposal is consistent with the data.

The mobility variations, though not as spectacular as the carrier-density changes in some samples, are nevertheless quite interesting. There has been much theoretical interest of late in critical magnetic scattering. Most of the theoretical comparison with experiment has been with Ni. The series of three curves in Figs. 9-11 show some interesting features that encourage comparison with EuO and other ferromagnetic semiconductors. The peaks are all rounded and all occur above the Curie point. Work done on CdCr_2Se_4 indicates this material exhibits the same effects, though they have not been emphasized in discussion. This mobility behavior implies that short-range order effects are important in conduction-electron scattering in these materials.

The magnetoresistance which we have observed in EuO is quite different from that observed in other ferromagnetic semiconductors. The magnetoresistance is associated with the structure in the ρ -vs- T curves, with the largest effects occurring near the elbow at 50°K and the mobility peak above the Curie point. The mobility peak is much more sensitive to low applied fields than the elbow at 50°K. Several features of the magnetoresistance structure

give confirmation to the assignments of the elbow as a carrier-density change phenomenon described by the proposed model and the peak as a mobility effect.

Data on the shift of the optical-absorption edge with magnetic field has been published by Busch and Wachter.³¹ As one would expect, the edge is lowered in energy under applied field. In terms of the model, this would shift the elbow to higher temperatures and decrease $d\rho/dT$ above the elbow. This is what is observed. A further point of interest is that, as the magnetic field is increased, the effect does not saturate. The elbow shift at 48 kG is roughly three times that at 16 kG. The same does not hold true of the mobility peak. The mobility well below the Curie point (near 60 °K) is not magnetically limited, so, for higher temperatures, the

maximum expected effect of an applied magnetic field is to increase the mobility to near the 60 °K level. This is quite similar to the behavior observed. The peak is mostly suppressed under a 12-kG applied field, and the incremental effect of the magnetic field decreases with increasing field.

ACKNOWLEDGMENTS

The authors wish to thank C. E. Hurwitz and J. A. Kafalas, with whom part of the work reported here was performed. N. Menyuk has made many susceptibility measurements which have helped to characterize the crystals. R. E. Fahey aided in crystal growth and W. H. Laswell prepared samples. Thanks are also due to S. von Molnar for many helpful discussions.

[†]This work was sponsored by the Department of the Air Force.

*Also Department of Electrical Engineering, Massachusetts Institute of Technology, Cambridge, Mass.

[†]Work based on a thesis submitted to the Massachusetts Institute of Technology in partial fulfillment of the requirements of Doctor of Science.

¹See S. Methfessel and D. C. Mattis, in *Handbuch der Physik*, edited by S. Flügge (Springer-Verlag, Berlin, 1968), Vol. XVIII/1, p. 384. EuO references include B. T. Matthias, R. M. Bozorth, and J. H. Van Vleck, *Phys. Rev. Letters* **7**, 160 (1961); B. E. Argyle and N. Miyata, *Phys. Rev.* **171**, 555 (1968).

²J. C. Suits, *Bull. Am. Phys. Soc.* **8**, 381 (1963).

³R. R. Heikes and C. W. Chen, *Physics* **1**, 159 (1964).

⁴S. von Molnar and S. Methfessel, *J. Appl. Phys.* **38**, 959 (1967).

⁵H. W. Lehmann, *Phys. Rev.* **163**, 488 (1967).

⁶P. -G. de Gennes and J. Friedel, *J. Phys. Chem. Solids* **4**, 171 (1958).

⁷C. Haas, *Phys. Rev.* **168**, 531 (1968).

⁸M. Fisher and J. Langer, *Phys. Rev. Letters* **22**, 1385 (1969).

⁹T. Kasuya and A. Yanase, *Rev. Mod. Phys.* **40**, 684 (1968); A. Yanase and T. Kasuya, *J. Appl. Phys.* **39**, 430 (1968); *J. Phys. Soc. Japan* **25**, 1025 (1968).

¹⁰See Ref. 1, p. 506.

¹¹C. F. Guerci and M. W. Shafer, *J. Appl. Phys.* **37**, 1406 (1966).

¹²T. B. Reed and R. E. Fahey, *J. Crystal Growth* **8**, 337 (1971).

¹³E. Kaldis, *J. Crystal Growth* **4**, 146 (1968).

¹⁴L. J. van der Pauw, *Philips Res. Rept.* **13**, 1 (1958).

¹⁵M. R. Oliver, J. A. Kafalas, J. O. Dimmock, and T. B. Reed, *Phys. Rev. Letters* **24**, 1064 (1970).

¹⁶S. von Molnar and M. W. Shafer, *J. Appl. Phys.* **41**, 1093 (1970).

¹⁷A. A. Samokhvalov, S. A. Ismailov, and A. Ya. Afanas'ev, *Fiz. Tverd. Tela* **10**, 425 (1968) [*Sov. Phys. Solid State* **10**, 334 (1968)].

¹⁸S. von Molnar, *IBM J. Res. Develop.* **14**, 269 (1970).

¹⁹M. R. Oliver, J. O. Dimmock, and T. B. Reed, *IBM J. Res. Develop.* **14**, 276 (1970).

²⁰S. von Molnar and T. Kasuya, *Phys. Rev. Letters* **21**, 1758 (1968).

²¹M. J. Freiser, F. Holtzberg, S. Methfessel, G. D. Pettit, M. W. Shafer, and J. C. Suits, *Helv. Phys. Acta* **41**, 832 (1968).

²²A. Amith and G. L. Gunsalus, *J. Appl. Phys.* **40**, 1020 (1969); A. Amith and L. R. Friedman, *Phys. Rev. B* **2**, 434 (1970).

²³J. Feinleib, W. J. Scouler, J. O. Dimmock, J. Hanus, T. B. Reed, and C. R. Pidgeon, *Phys. Rev. Letters* **22**, 1385 (1969).

²⁴S. von Molnar, in *Proceedings of the Tenth International Conference on Physics of Semiconductors* (U.S. Atomic Energy Commission, Oak Ridge, Tenn., 1970), p. 233.

²⁵W. Baltensperger, *J. Appl. Phys.* **41**, 1052 (1970).

²⁶J. D. Axe, *J. Phys. Chem. Solids* **30**, 1403 (1969).

²⁷P. B. Phipps, *Bull. Am. Phys. Soc.* **15**, 1613 (1970).

²⁸C. Haas, A. M. J. G. Run, P. F. Bongers, and W. Albers, *Solid State Commun.* **5**, 657 (1967).

²⁹P. Wachter, *Solid State Commun.* **7**, 693 (1969).

³⁰F. Holtzberg, T. R. McGuire, S. Methfessel, and J. C. Suits, *Phys. Rev. Letters* **13**, 18 (1964).

³¹G. Busch and P. Wachter, *Physik Kondensierten Materie* **5**, 232 (1966).